

Nuclear fission

Contributed by: John R. Huizenga

Publication year: 2014

An extremely complex nuclear reaction representing a cataclysmic division of an atomic nucleus into two nuclei of comparable mass. This rearrangement or division of a heavy nucleus may take place naturally (spontaneous fission) or under bombardment with neutrons, charged particles, gamma rays, or other carriers of energy (induced fission). Although nuclei with mass number A of approximately 100 or greater are energetically unstable against division into two lighter nuclei, the fission process has a small probability of occurring, except with the very heavy elements. Even for these elements, in which the energy release is of the order of 2×10^8 eV, the lifetimes against spontaneous fission are reasonably long. *See also:* NUCLEAR REACTION.

Liquid-drop model

The stability of a nucleus against fission is most readily interpreted when the nucleus is viewed as being analogous to an incompressible and charged liquid drop with a surface tension. Such a droplet is stable against small deformations when the dimensionless fissility parameter X in Eq. (1)

$$X = \frac{(\text{charge})^2}{10 \times \text{volume} \times \text{surface tension}} \quad (1)$$

is less than unity, where the charge is in esu, the volume is in cm^3 , and the surface tension is in ergs/cm^2 . The fissility parameter is given approximately, in terms of the charge number Z and mass number A , by the relation $X = Z^2/47A$.

Long-range Coulomb forces between the protons act to disrupt the nucleus, whereas short-range nuclear forces, idealized as a surface tension, act to stabilize it. The degree of stability is then the result of a delicate balance between the relatively weak electromagnetic forces and the strong nuclear forces. Although each of these forces results in potentials of several hundred megaelectronvolts, the height of a typical barrier against fission for a heavy nucleus, because they are of opposite sign but do not quite cancel, is only 5 or 6 MeV. Investigators have used this charged liquid-drop model with great success in describing the general features of nuclear fission and also in reproducing the total nuclear binding energies. *See also:* NUCLEAR BINDING ENERGY; NUCLEAR STRUCTURE; SURFACE TENSION.

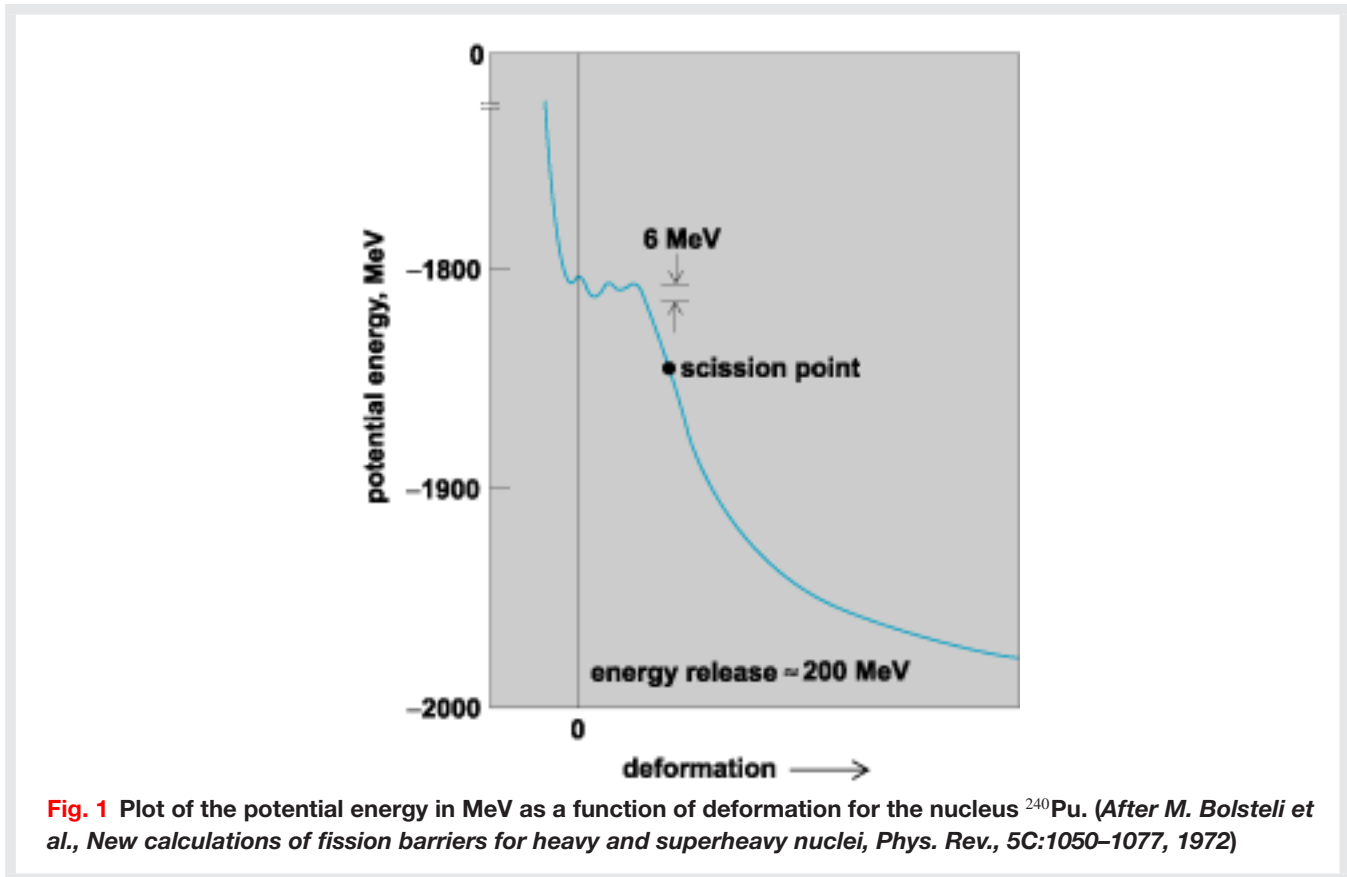
Shell corrections

The general dependence of the potential energy on the fission coordinate representing nuclear elongation or deformation for a heavy nucleus such as ^{240}Pu is shown in **Fig. 1**. The expanded scale used in this figure shows the large decrease in energy of about 200 MeV as the fragments separate to infinity. It is known that ^{240}Pu is deformed in its ground state, which is represented by the lowest minimum of -1813 MeV near zero deformation. This energy represents the total nuclear binding energy when the zero of potential energy is the energy of the individual nucleons at a separation of infinity. The second minimum to the right of zero deformation illustrates structure introduced in the fission barrier by shell corrections, that is, corrections dependent upon microscopic behavior of the individual nucleons, to the liquid-drop mass. Although shell corrections introduce small wiggles in the potential-energy surface as a function of deformation, the gross features of the surface are reproduced by the liquid-drop model. Since the typical fission barrier is only a few megaelectronvolts, the magnitude of the shell correction need only be small for irregularities to be introduced into the barrier. This structure is schematically illustrated for a heavy nucleus by the double-humped fission barrier in **Fig. 2**, which represents the region to the right of zero deformation in **Fig. 1** on an expanded scale. The fission barrier has two maxima and a rather deep minimum in between. For comparison, the single-humped liquid-drop barrier is also schematically illustrated. The transition in the shape of the nucleus as a function of deformation is represented in the upper part of the figure.

Double-humped barrier

The developments which led to the proposal of a double-humped fission barrier were triggered by the experimental discovery of spontaneously fissionable isomers by S. M. Polikanov and colleagues in the Soviet Union and by V. M. Strutinsky's pioneering theoretical work on the binding energy of nuclei as a function of both nucleon number and nuclear shape. The double-humped character of the nuclear potential energy as a function of deformation arises, within the framework of the Strutinsky shell-correction method, from the superposition of a macroscopic smooth liquid-drop energy and a shell-correction energy obtained from a microscopic single-particle model. Oscillations occurring in this shell correction as a function of deformation lead to two minima in the potential energy, shown in **Fig. 2**, the normal ground-state minimum at a deformation of β_1 and a second minimum at a deformation of β_2 . States in these wells are designated class I and class II states, respectively. Spontaneous fission of the ground state and isomeric state arises from the lowest-energy class I and class II states, respectively. *See also:* NUCLEAR ISOMERISM.

The calculation of the potential-energy curve illustrated in **Fig. 1** may be summarized as follows, The smooth potential energy obtained from a macroscopic (liquid-drop) model is added to a fluctuating potential energy representing the shell corrections, and to the energy associated with the pairing of like nucleons (pairing energy), derived from a non-self-consistent microscopic model. The calculation of these corrections requires several steps: (1) specification of the geometrical shape of the nucleus, (2) generation of a single-particle



potential related to its shape, (3) solution of the Schrödinger equation, and (4) calculation from these single-particle energies of the shell and pairing energies.

The oscillatory character of the shell corrections as a function of deformation is caused by variations in the single-particle level density in the vicinity of the Fermi energy. For example, the single-particle levels of a pure harmonic oscillator potential arrange themselves in bunches of highly degenerate shells at any deformation for which the ratio of the major and minor axes of the spheroidal equipotential surfaces is equal to the ratio of two small integers. Nuclei with a filled shell, that is, with a level density at the Fermi energy that is smaller than the average, will then have an increased binding energy compared to the average, because the nucleons occupy deeper and more bound states; conversely, a large level density is associated with a decreased binding energy. It is precisely this oscillatory behavior in the shell correction that is responsible for spherical or deformed ground states and for the secondary minima in fission barriers, as illustrated in Fig. 2. *See also:* NONRELATIVISTIC QUANTUM THEORY.

More detailed theoretical calculations based on this macroscopic-microscopic method have revealed additional features of the fission barrier. In these calculations the potential energy is regarded as a function of several different modes of deformation. The outer barrier B (Fig. 2) is reduced in energy for shapes with pronounced

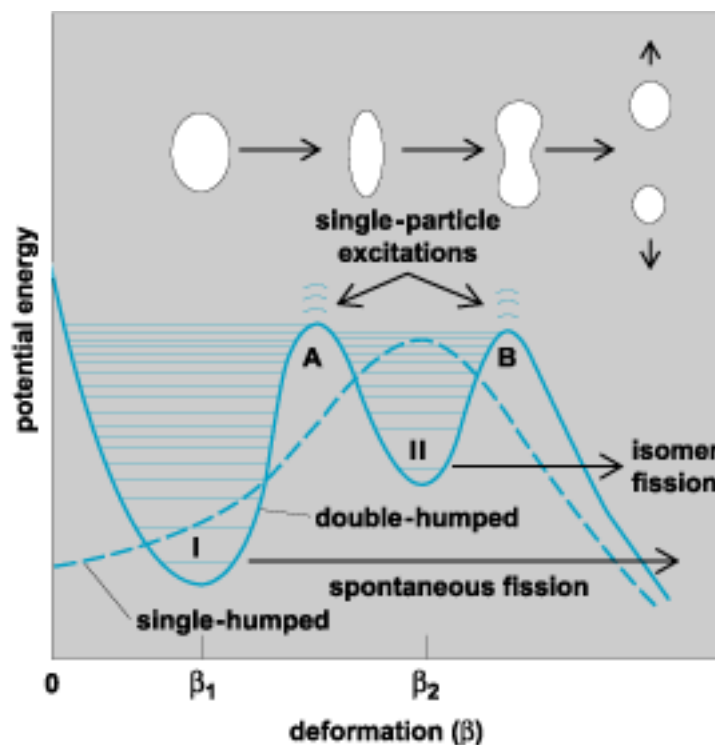


Fig. 2 Schematic plots of single-humped fission barrier of liquid-drop model and double-humped barrier introduced by shell corrections. (After J. R. Huizenga, *Nuclear fission revisited*, *Science*, 168:1405–1413, 1970)

left-right asymmetry (pear shapes), whereas the inner barrier A and deformations in the vicinity of the second minimum are stable against such mass asymmetric degrees of freedom. Similar calculations of potential-energy landscapes reveal the stability of the second minimum against gamma deformations, in which the two small axes of the spheroidal nucleus become unequal, that is, the spheroid becomes an ellipsoid.

Experimental consequences

The observable consequences of the double-humped barrier have been reported in numerous experimental studies. In the actinide region, more than 30 spontaneously fissionable isomers have been discovered between uranium and berkelium, with half-lives ranging from 10^{-11} to 10^{-2} s. These decay rates are faster by 20 to 30 orders of magnitude than the fission half-lives of the ground states, because of the increased barrier tunneling probability (Fig. 2). Several cases in which excited states in the second minimum decay by fission are also known. Normally these states decay within the well by gamma decay; however, if there is a hindrance in gamma decay due to spin, the state (known as a spin isomer) may undergo fission instead.

Qualitatively, the fission isomers are most stable in the vicinity of neutron numbers 146 to 148, a value in good agreement with macroscopic-microscopic theory. For elements above berkelium, the half-lives become too short to be observable with available techniques; and for elements below uranium, the prominent decay is through

barrier A into the first well, followed by gamma decay. It is difficult to detect this competing gamma decay of the ground state in the second well (called a shape isomeric state), but identification of the gamma branch of the 200-ns ^{238}U shape isomer has been reported. *See also:* RADIOACTIVITY.

Direct evidence of the second minimum in the potential-energy surface of the even-even nucleus ^{240}Pu has been obtained through observations of the E2 transitions within the rotational band built on the isomeric 0^+ level. The rotational constant (which characterizes the spacing of the levels and is expected to be inversely proportional to the effective moment of inertia of the nucleus) found for this band is less than one-half that for the ground state and confirms that the shape isomers have a deformation β_2 much larger than the equilibrium ground-state deformation β_1 . From yields and angular distributions of fission fragments from the isomeric ground state and low-lying excited states, some information has been derived on the quantum numbers of specific single-particle states of the deformed nucleus (Nilsson single-particle states) in the region of the second minimum.

At excitation energies in the vicinity of the two barrier tops, measurements of the subthreshold neutron fission cross sections of several nuclei have revealed groups of fissioning resonance states with wide energy intervals between each group where no fission occurs. Such a spectrum is illustrated in **Fig. 3a**, where the subthreshold fission cross section of ^{240}Pu is shown for neutron energies between 500 and 3000 eV. As shown in **Fig. 3b**, between the fissioning resonance states there are many other resonance states, known from data on the total neutron cross sections, which have negligible fission cross sections. Such structure is explainable in terms of the double-humped fission barrier and is ascribed to the coupling between the compound states of normal density in the first well to the much less dense states in the second well. This picture requires resonances of only one spin to appear within each intermediate structure group illustrated in **Fig. 3a**. In an experiment using polarized neutrons on a polarized ^{237}Np target, it was found that all nine fine-structure resonances of the 40-eV group have the same spin and parity: $I = 3^+$. Evidence has also been obtained for vibrational states in the second well from neutron (n,f) and deuteron stripping (d,pf) reactions at energies below the barrier tops (f indicates fission of the nucleus). *See also:* NEUTRON SPECTROMETRY.

A. Bohr suggested that the angular distributions of the fission fragments are explainable in terms of the transition-state theory, which describes a process in terms of the states present at the barrier deformation. The theory predicts that the cross section will have a steplike behavior for energies near the fission barrier, and that the angular distribution will be determined by the quantum numbers associated with each of the specific fission channels. The theoretical angular distribution of fission fragments is based on two assumptions. First, the two fission fragments are assumed to separate along the direction of the nuclear symmetry axis so that the angle θ between the direction of motion of the fission fragments and the direction of motion of the incident bombarding particle represents the angle between the body-fixed axis (the long axis of the spheroidal nucleus) and the space-fixed axis (some specified direction in the laboratory, in this case the direction of motion of the incident particle). Second, it is assumed that during the transition from the saddle point (corresponding to the top of the barrier) to scission (the division of the nucleus into two fragments) the Coriolis forces do not change the value of

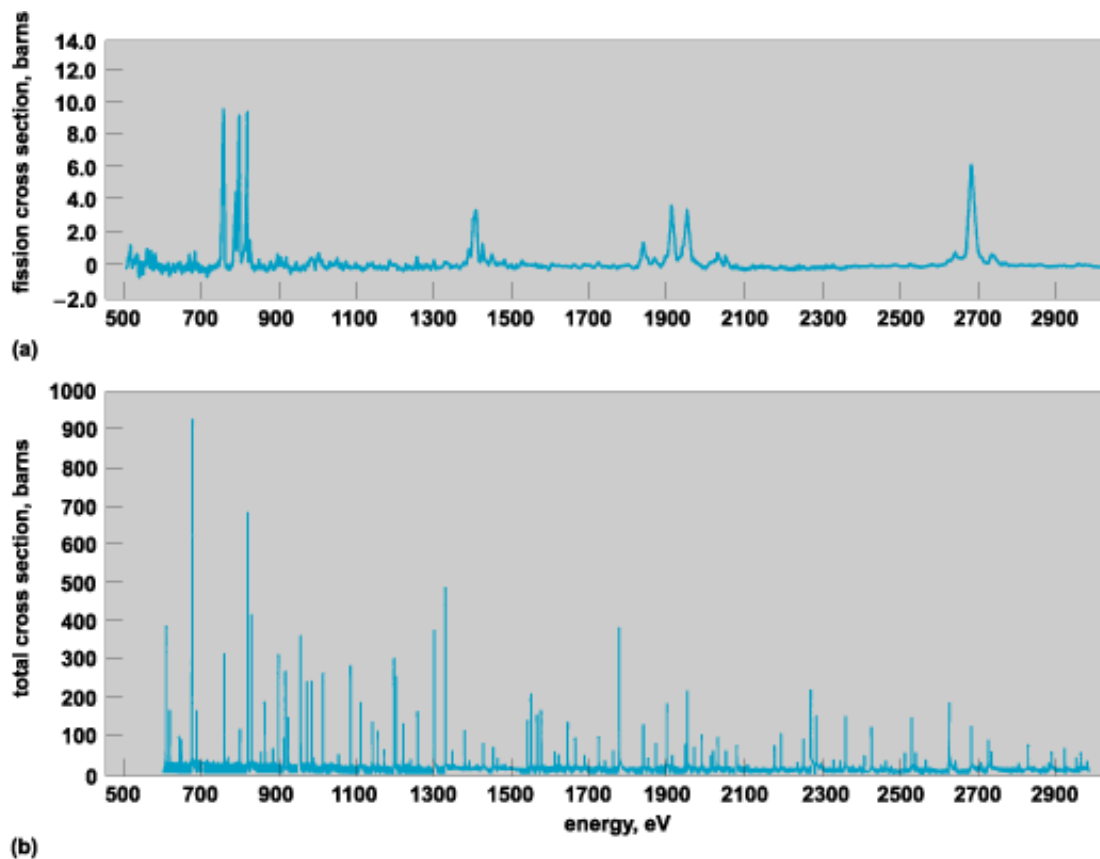


Fig. 3 Grouping of fission resonances demonstrated by (a) the neutron fission cross section of ^{240}Pu and (b) the total neutron cross section. (After V. M. Strutinsky and H. C. Pauli, *Shell-structure effects in the fissioning nucleus*, *Proceedings of the 2d IAEA Symposium on Physics and Chemistry of Fission*, Vienna, pp. 155–177, 1969)

K (where K is the projection of the total angular momentum I on the nuclear symmetry axis) established at the saddle point.

In several cases, low-energy photofission and neutron fission experiments have shown evidence of a double-humped barrier. In the case of two barriers, the question arises as to which of the two barriers A or B is responsible for the structure in the angular distributions. For light actinide nuclei like thorium, the indication is that barrier B is the higher one, whereas for the heavier actinide nuclei, the inner barrier A is the higher one. The heights of the two barriers themselves are most reliably determined by investigating the probability of induced fission over a range of several mega-electronvolts in the threshold region. Many direct reactions have been used for this purpose, for example, (d,pt) , (t,pf) , and $(^3\text{He},df)$. There is reasonably good agreement between the experimental and theoretical barriers. The theoretical barriers are calculated with realistic single-particle potentials and include the shell corrections.

Fission probability

The cross section for particle-induced fission $\sigma(y, f)$ represents the cross section for a projectile y to react with a nucleus and produce fission, as shown by Eq. (2).

$$\sigma(y, f) = \sigma_R(y) \frac{\Gamma_f}{\Gamma_t} \quad (2)$$

The quantities $\sigma_R(y)$, Γ_f , and Γ_t are the total reaction cross sections for the incident particle y , the fission width, and the total level width, respectively, where $\Gamma_t = \Gamma_f + \Gamma_n + \Gamma_\gamma + \dots$ is the sum of all partial-level widths. All the quantities in Eq. (2) are energy-dependent. Each of the partial widths for fission, neutron emission, radiation, and so on, is defined in terms of a mean lifetime τ for that particular process, for example, $\Gamma_f = \hbar/\tau_f$. Here \hbar , the action quantum, is Planck's constant divided by 2π and is numerically equal to $1.0546 \times 10^{-34} \text{ J s} = 0.66 \times 10^{-15} \text{ eV s}$. The fission width can also be defined in terms of the energy separation D of successive levels in the compound nucleus and the number of open channels in the fission transition nucleus (paths whereby the nucleus can cross the barrier on the way to fission), as given by expression (3),

$$\Gamma_f(I) = \frac{D(I)}{2\pi} \sum_i N_{fi} \quad (3)$$

where I is the angular momentum and i is an index labeling the open channels N_{fi} . The contribution of each fission channel to the fission width depends upon the barrier transmission coefficient, which, for a two-humped barrier (see Fig. 2), is strongly energy-dependent. This results in an energy-dependent fission cross section which is very different from the total cross section shown in Fig. 3 for ^{240}Pu .

When the incoming neutron has low energy, the likelihood of reaction is substantial only when the energy of the neutron is such as to form the compound nucleus in one or another of its resonance levels (Fig. 3*b*). The requisite sharpness of the “tuning” of the energy is specified by the total level width Γ . The nuclei ^{233}U , ^{235}U , and ^{239}Pu have a very large cross section to take up a slow neutron and undergo fission (see **table**) because both their absorption cross section and their probability for decay by fission are large. The probability for fission decay is high because the binding energy of the incident neutron is sufficient to raise the energy of the compound nucleus above the fission barrier. The very large, slow neutron fission cross sections of these isotopes make them important fissile materials in a chain reactor. *See also:* CHAIN REACTION (PHYSICS); REACTOR PHYSICS.

Cross sections for neutrons of thermal energy to produce fission or undergo capture in the principal nuclear species, and neutron yields from these nuclei*

Nucleus	Cross section for fission, σ_f , 10^{-24} cm ²	σ_f plus cross section for radiative capture, σ_γ	Ratio, $1 + \alpha$	Number of neutrons released per fission, ν	Number of neutrons released per slow neutron captured, $\eta = \nu/(1 + \alpha)$
²³³ U	525 ± 2	573 ± 2	1.093 ± 0.003	2.50 ± 0.01	2.29 ± 0.01
²³⁵ U	577 ± 1	678 ± 2	1.175 ± 0.002	2.43 ± 0.01	2.08 ± 0.01
²³⁹ Pu	741 ± 4	1015 ± 4	1.370 ± 0.006	2.89 ± 0.01	2.12 ± 0.01
²³⁸ U	0	2.73 ± 0.04			0
Natural uranium	4.2	7.6	1.83	2.43 ± 0.01	1.33

*Data from *Brookhaven National Laboratory 325*, 2d ed., suppl. no. 2, vol. 3, 1965. The data presented are the recommended or least-square values published in this reference for 0.0253-eV neutrons.

Scission

The scission configuration is defined in terms of the properties of the intermediate nucleus just prior to division into two fragments. In heavy nuclei the scission deformation is much larger than the saddle deformation at the barrier, and it is important to consider the dynamics of the descent from saddle to scission. One of the important questions in the passage from saddle to scission is the extent to which this process is adiabatic with respect to the particle degrees of freedom. As the nuclear shape changes, it is of interest to investigators to know the probability for the nucleons to remain in the lowest-energy orbitals. If the collective motion toward scission is very slow, the single-particle degrees of freedom continually readjust to each new deformation as the distortion proceeds. In this case, the adiabatic model is a good approximation, and the decrease in potential energy from saddle to scission appears in collective degrees of freedom at scission, primarily as kinetic energy associated with the relative motion of the nascent fragments.

On the other hand, if the collective motion between saddle and scission is so rapid that equilibrium is not attained, there will be a transfer of collective energy into nucleonic excitation energy. Such a nonadiabatic model, in which collective energy is transferred to single-particle degrees of freedom during the descent from saddle to scission, is usually referred to as the statistical theory of fission. *See also*: PERTURBATION (QUANTUM MECHANICS).

The experimental evidence indicates that the saddle to scission time is somewhat intermediate between these two extreme models. The dynamic descent of a heavy nucleus from saddle to scission depends upon the nuclear viscosity. A viscous nucleus is expected to have a smaller translational kinetic energy at scission and a more elongated scission configuration. Experimentally, the final translational kinetic energy of the fragments at infinity, which is related to the scission shape, is measured. Hence, in principle, it is possible to estimate the nuclear viscosity coefficient by comparing the calculated dependence upon viscosity of fission-fragment kinetic energies with experimental values. The viscosity of nuclei is an important nuclear parameter which also plays an important role in collisions of very heavy ions.

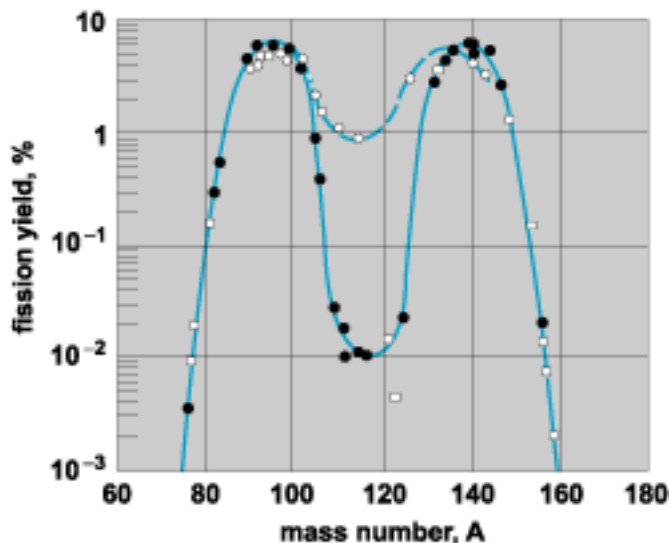


Fig. 4 Mass distribution of fission fragments formed by neutron-induced fission of $^{235}\text{U} + n = ^{236}\text{U}$ when neutrons have thermal energy, solid curve (*Plutonium Project Report, Rev. Mod. Phys.*, 18:539, 1964), and 14-MeV energy, broken curve (based on R. W. Spence, *Brookhaven National Laboratory, AEC-BNL (C-9)*, 1949). Quantity plotted is $100 \times (\text{number of fission decay chains formed with given mass})/(\text{number of fissions})$.

The mass distribution from the fission of heavy nuclei is predominantly asymmetric. For example, division into two fragments of equal mass is about 600 times less probable than division into the most probable choice of fragments when ^{235}U is irradiated with thermal neutrons. When the energy of the neutrons is increased, symmetric fission (**Fig. 4**) becomes more probable. In general, heavy nuclei fission asymmetrically to give a heavy fragment of approximately constant mean mass number 139 and a corresponding variable-mass light fragment (**Fig. 5**). These experimental results have been difficult to explain theoretically. Calculations of potential-energy surfaces show that the second barrier (B in **Fig. 2**) is reduced in energy by up to 2 or 3 MeV, if octupole deformations (pear shapes) are included. Hence, the theoretical calculations show that mass asymmetry is favored at the outer barrier, although direct experimental evidence supporting the asymmetric shape of the second barrier is very limited. It is not known whether the mass asymmetric energy valley extends from the saddle to scission; and the effect of dynamics on mass asymmetry in the descent from saddle to scission has not been determined. Experimentally, as the mass of the fissioning nucleus approaches $A \approx 260$, the mass distribution approaches symmetry. This result is qualitatively in agreement with theory.

A nucleus at the scission configuration is highly elongated and has considerable deformation energy. The influence of nuclear shells on the scission shape introduces structure into the kinetic energy and neutron-emission yield as a function of fragment mass. The experimental kinetic energies for the neutron-induced fission of ^{233}U , ^{235}U , and ^{239}Pu have a pronounced dip as symmetry is approached, as shown in **Fig. 6**. (This dip is slightly exaggerated in the figure because the data have not been corrected for fission fragment scattering.) The variation in the neutron yield as a function of fragment mass for these same nuclei (**Fig. 7**) has a “saw-toothed”

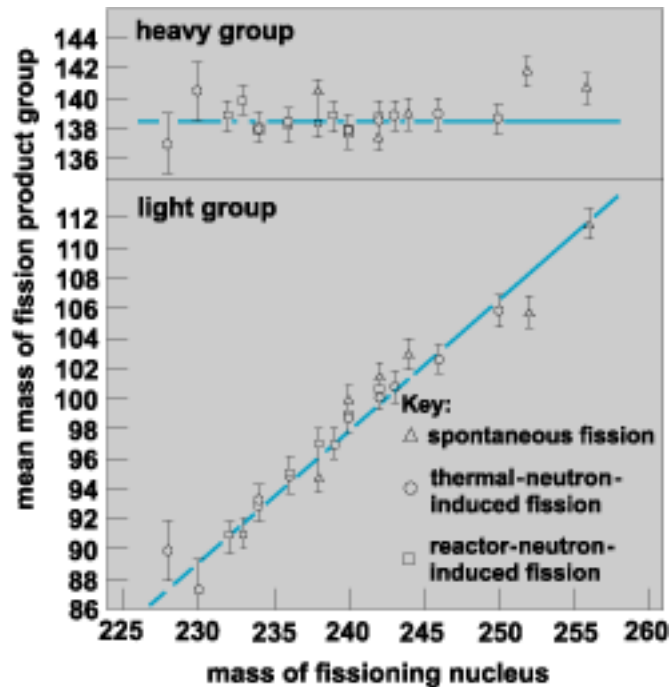


Fig. 5 Average masses of the light- and heavy-fission product groups as a function of the masses of the fissioning nucleus. Energy spectrum of reactor neutrons is that associated with fission. (After K. F. Flynn et al., *Distribution of mass in the spontaneous fission of ^{256}Fm* , *Phys. Rev.*, 5C:1725–1729, 1972)

shape which is asymmetric about the mass of the symmetric fission fragment. Both these phenomena are reasonably well accounted for by the inclusion of closed-shell structure into the scission configuration.

A number of light charged particles (for example, isotopes of hydrogen, helium, and lithium) have been observed to occur, with low probability, in fission. These particles are believed to be emitted very near the time of scission. Available evidence also indicates that neutrons are emitted at or near scission with considerable frequency.

Postscission phenomena

After the fragments are separated at scission, they are further accelerated as the result of the large Coulomb repulsion. The initially deformed fragments collapse to their equilibrium shapes, and the excited primary fragments lose energy by evaporating neutrons. After neutron emission, the fragments lose the remainder of their energy by gamma radiation, with a life-time of about 10^{-11} s. The kinetic energy and neutron yield as a function of mass are shown in Figs. 6 and 7. The variation of neutron yield with fragment mass is directly related to the fragment excitation energy. Minimum neutron yields are observed for nuclei near closed shells because of the resistance to deformation of nuclei with closed shells. Maximum neutron yields occur for fragments that are “soft” toward nuclear deformation. Hence, at the scission configuration, the fraction of the deformation energy stored in each fragment depends on the shell structure of the individual fragments. After scission, this

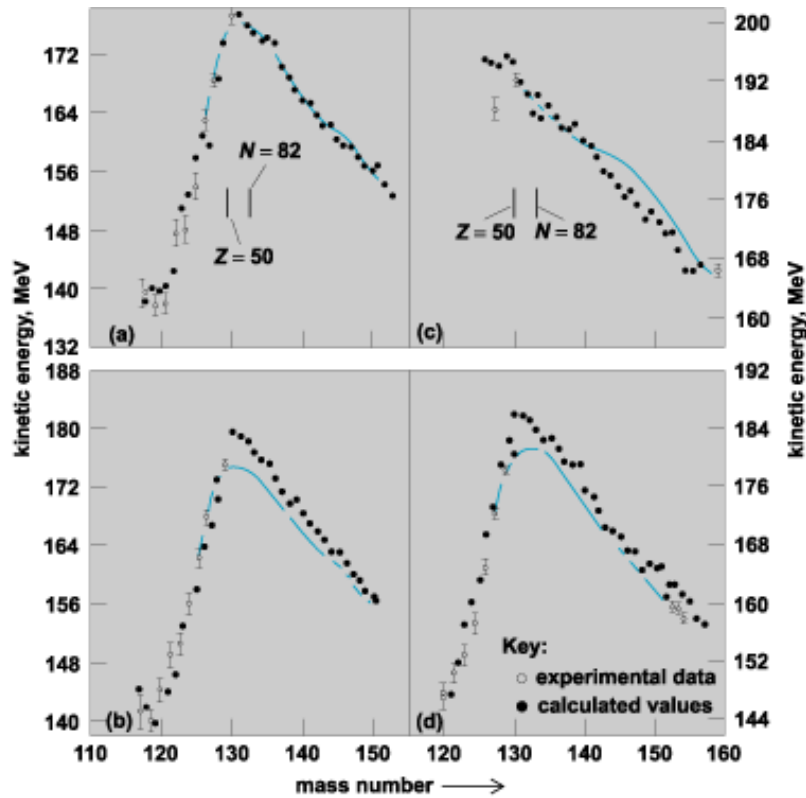


Fig. 6 Average total kinetic energy of fission fragments as a function of heavy fragment mass for fission of (a) ^{235}U , (b) ^{233}U , (c) ^{252}Cf , and (d) ^{239}Pu . Curves indicate experimental data. (After J. C. D. Milton and J. S. Fraser, *Time-of-flight fission studies on ^{233}U , ^{235}U and ^{239}Pu* , *Can. J. Phys.*, 40:1626–1663, 1962)

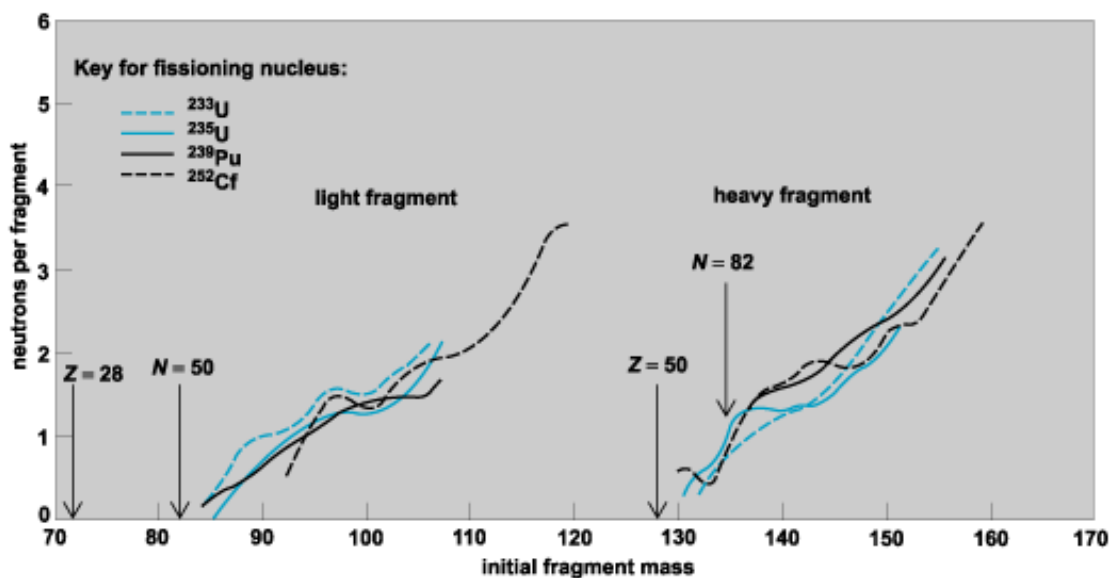


Fig. 7 Neutron yields as a function of fragment mass for four types of fission as determined from mass-yield data. Approximate initial fragment masses corresponding to various neutron and proton “magic numbers” N and Z are indicated. (After J. Terrell, *Neutron yields from individual fission fragments*, *Phys. Rev.*, 127:880–904, 1962)

deformation energy is converted to excitation energy, and hence, the neutron yield is directly correlated with the fragment shell structure. This conclusion is further supported by the correlation between the neutron yield and the final kinetic energy. Closed shells result in a larger Coulomb energy at scission for fragments that have a smaller deformation energy and a smaller number of evaporated neutrons.

After the emission of the prompt neutrons and gamma rays, the resulting fission products are unstable against beta decay. For example, in the case of thermal neutron fission of ^{235}U , each fragment undergoes on the average about three beta decays before it settles down to a stable nucleus. For selected fission products (for example, ^{87}Br and ^{137}I) beta decay leaves the daughter nucleus with excitation energy exceeding its neutron binding energy. The resulting delayed neutrons amount, for thermal neutron fission of ^{235}U , to about 0.7% of all the neutrons that are given off in fission. Although small in number, these neutrons are quite important in stabilizing nuclear chain reactions against sudden minor fluctuations in reactivity. *See also:* DELAYED NEUTRON; NEUTRON; THERMAL NEUTRONS.

John R. Huizenga

Bibliography

P. David (ed.), *Dynamics of Nuclear Fission and Related Collective Phenomena, Proceedings*, Bad Honnef, Germany, Springer, Berlin, 1982

J. Kliman, M. G. Itkis, and Š. Gmuca (eds.), *Dynamical Aspects of Nuclear Fission: Proceedings of the 6th International Conference*, World Scientific, Singapore, 2008

J. Krištiak and B. I. Pustyl'nik (eds.), *Dynamical Aspects of Nuclear Fission: Proceedings of the 2d International Conference*, Joint Institute for Nuclear Research, Dubna, Russia, 1994

H. Marten and D. Seelinger (eds.), *Physics and Chemistry of Fission*, Nova Science, New York, 1992

R. Vandenbosch and J. R. Huizenga, *Nuclear Fission*, Academic Press, New York, 1973

Additional Readings

S. Panebianco et al., Role of deformed shell effects on the mass asymmetry in nuclear fission of mercury isotopes, *Phys. Rev. C*, 86(6):064601, 2012 DOI: <http://doi.org/10.1103/PhysRevC.86.064601>

J. Randrup and P. Möller, Brownian shape motion on five-dimensional potential-energy surfaces: Nuclear fission-fragment mass distributions, *Phys. Rev. Lett.*, 106(13):132503, 2011
DOI: <http://doi.org/10.1103/PhysRevLett.106.132503>

A. Vértes et al. (eds.), *Handbook of Nuclear Chemistry: Basics of Nuclear Science*, 2d ed., vol. 1, Springer Science+Business Media, Dordrecht, Netherlands, 2011